Collective excitations of the hybrid atomic-molecular Bose-Einstein condensates

Moumita Gupta* and Krishna Rai Dastidar†
Department of Spectroscopy, Indian Association for the Cultivation of Science, Kolkata 700032, India
(Received 3 March 2010; published 24 June 2010)

We investigate the low-energy excitations of the spherically and axially trapped atomic Bose-Einstein condensate coupled to a molecular Bose gas by coherent Raman transitions. We apply the sum-rule approach of many-body response theory to derive the low-lying collective excitation frequencies of the hybrid atom-molecular system. The atomic and molecular ground-state densities obtained in Gross-Pitaevskii and modified Gross-Pitaevskii (including the higher order Lee-Huang-Yang term in interatomic interaction) approaches are used to find out the individual energy components and hence the excitation frequencies. We obtain different excitation energies for different angular momenta and study their characteristic dependence on the effective Raman detuning, the scattering length for atom-atom interaction, and the intensities of the coupling lasers. We show that the inclusion of the higher-order nonlinear interatomic interaction in modified Gross-Pitaevskii approach introduces significant corrections to the ground-state properties and the excitation frequencies both for axially and spherically trapped coupled ^{87}Rb condensate system with the increase in the *s*-wave scattering length (for peak gas-parameter $\geqslant 10^{-3}$). It has been shown that the excitation frequencies decrease with the increase in the effective Raman detuning as well as the *s*-wave scattering length, whereas excitation frequencies increase with the increase in the atom-molecular coupling strength. The frequencies in modified Gross-Pitaevskii approximation exhibit an upward trend after a certain value of scattering length and also largely deviate from the Gross-Pitaevskii results with the increase in *s*-wave scattering length. The strong dependence of excitation frequencies on the laser intensities used for Raman transitions manifests the role of atom-molecular coupling strength on the control of collective excitations. The collective excitation frequencies for the hybrid atom-molecular BEC differ significantly from the excitation frequencies of a pure atomic BEC system when the atom-to-molecule conversion efficiency increases due to the decrease in the effective Raman detuning and increase in the atom-molecule coupling strength.

DOI: 10.1103/PhysRevA.81.063631 PACS number(s): 03.75.Hh, 34.50.Cx, 03.65.Db

I. INTRODUCTION

Producing ultracold molecules from the atoms in a Bose-Einstein condensate (BEC) gives a new dimension to the emerging science of BECs [1–3]. Conversion of atomic BECs to a molecular BEC in the process of both magnetic Feshbach resonance and photoassociation generates a coherence in the coupled atomic-molecular condensates and this becomes evident in the dynamics of the system [4–9] as shown in theoretical studies. Using coupled Gross-Pitaevskii- (GP) type equations the dynamic properties of the molecular condensate coupled with the atomic BEC via Raman photoassociation have been studied [6,7]. Theoretical investigations of the effects of modified GP (MGP) theory on the coherent dynamics of the coupled system and on the atom-to-molecule conversion efficiency have been already discussed [8] in the large-gas-parameter region. The dependence of the atom-molecule coherence and the atom-to-molecule conversion efficiency on the intensities of the coupling lasers has also been demonstrated [9]. It is also expected that for large values of gas parameter the changes due to higher-order nonlinearity (in modified GP approach) will be reflected in the frequencies of collective oscillations of the system. In the past, the collective excitations of a BEC in a dilute atomic gas have been observed experimentally [10–13] and the Gross-Pitaevskii (GP) equation has been used to describe the dynamic process of the low-lying collective excitations of the trapped atomic Bose gas [14–16]. The intensive study of the behavior of elementary excitations of a BEC has been done previously at zero and finite temperature [17–20]. The first corrections (Lee-Huang-Yang term) to the collective frequencies and excitation spectrum of the atomic Bose gas have been considered earlier [21,22]. Although the corrections are small ($\sim$1%) in case of weakly interacting gas [21], they might be visible experimentally where the accuracy of measurements is much higher [11]. Corrections to the collective excitation frequencies of spherically and axially trapped atomic BEC due to the higher order nonlinearity have been estimated by solving GP and modified GP (MGP) equations numerically and also analytically within modified Thomas-Fermi approximation [23–25]. The behavior of the collective excitation modes of the hybrid atom-molecular system as a function of the Feshbach detuning in strong and weak resonance limit has been studied parametrically [26]. The main aim of this article is to study the dependence of collective excitation frequencies of the hybrid atom-molecular system on the effective Raman detuning and atom-molecular coupling strength as well as on the *s*-wave scattering length. In addition to this the Lee-Huang-Yang (LHY) correction term giving rise to higher-order nonlinearity in atom-atom interaction has been taken into account for the large gas parameter. The effect of higher-order nonlinearity in molecule-molecule and atom-molecule interactions has not been considered here. We will derive the expressions for the frequencies of low-energy collective excitations of the atom-molecular system coupled by two-photon Raman photoassociation using sum-rule approach

*mou_mita_81@yahoo.co.in
†krishna_raidastidar@yahoo.co.in

of many-body response theory [27,28] and investigate the dependence of the excitation frequencies as a function of the effective Raman detuning, the scattering length of atom-atom interactions, and the intensities of the coupling lasers in GP and MGP approaches. Previously the sum-rule approach has been used to derive the different modes of excitation spectrum of interacting atomic Bose gases [23,24,29–32]. In this study the stationary state densities of atoms and molecules for the axially and spherically trapped hybrid system have been calculated by solving the static GP and MGP equations numerically, the knowledge of which is required to obtain the excitation frequencies in sum-rule approach. It is well known that the higher-order nonlinear effect becomes prominent when the peak gas-parameter $x_{pk} \geqslant 10^{-3}$ ($x_{pk} = n_{pk}a^3$, where n_{pk} is the peak density of the system and a is the s-wave scattering length). In this work we have found that MGP and GP results differ significantly for large values of s-wave scattering length (for $x_{pk} \geqslant 10^{-3}$). Furthermore, this study also demonstrates the significant difference between the excitation frequencies for the hybrid atom-molecular condensates and the frequencies for a pure atomic BEC when the effective Raman detuning decreases and the atom-molecular coupling strength increases.

The article is organized as follows. In subsection II A we first define our model and give the time-independent coupled GP and MGP equations of motion to describe the stationary state of the system neglecting the effect of particle loss. In subsection II B the frequencies of collective oscillations have been derived in the sum-rule approach in terms of static densities obtained from coupled GP and MGP equations given in subsection II A. In Sec. III, we give the results for low-energy excitation frequencies as a function of the effective Raman detuning, the atom-atom scattering length, and the intensities of coupling lasers. Finally, we conclude in Sec. IV.

II. THEORY

A. Stationary states

Figure 1 sketches the process of Raman photoassociation in which the atomic BEC ground state ($|a\rangle$) with total energy $2E_1$ [described by potential $V_g(R)$] is coupled to a group of excited molecular states ($|v\rangle$) [each with energy E_v in a potential $V_e(R)$] by a laser field with intensity I_1 and frequency

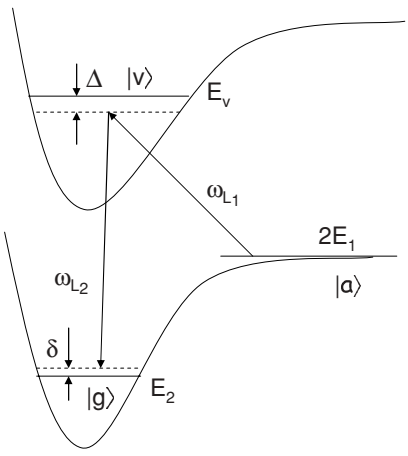

FIG. 1. Diagrammatic representation of Raman photoassociation.

ω_{L_1}. The excited molecules are then coupled to a condensed molecular ground state ($|g\rangle$) of energy E_2 by another laser field with intensity I_2 and frequency ω_{L_2}. The process of Raman coupling becomes resonant when the two-photon Raman detuning $\delta = (2E_1 - E_2)/\hbar - (\omega_{L_2} - \omega_{L_1})$ is zero. Two laser fields $\mathbf{E}_i = \mathbf{E}_{0i}\cos(\omega_i t)(i = 1,2)$ couple the ground state with the electronically excited state with Rabi frequencies $\Omega_i = |\mathbf{d}_i \cdot \mathbf{E}_{0i}|/\hbar$, where $\mathbf{d}_i$ is the molecular electric dipole matrix elements for free-bound and bound-bound transitions, respectively. The free-bound (Ω_1) and bound-bound (Ω_2) Rabi frequencies depend on the laser intensities I_1 and I_2, respectively: $\Omega_i \propto \sqrt{I_i}$. The atom-molecular Raman coupling ($\chi \propto \Omega_1\Omega_2$) creates a molecular condensate component in the presence of an atomic condensate and is given by the equation

$$\frac{\chi}{\hbar} = -\frac{\Omega_1\Omega_2}{2\sqrt{2}} \sum_v \frac{I_{1,v}I_{2,v}}{\Delta_v}, \tag{1}$$

where $I_{j,v}$ are the free-bound ($j = 1$) and bound-bound ($j = 2$) Franck-Condon factors. The relevant detunings are defined as

$$\Delta_v = (E_v - 2E_1)/\hbar - \omega_{L_1}, \quad \Delta_v^{(1)} = (E_v - 2E_1)/\hbar - \omega_{L_2},$$

and

$$\Delta_v^{(2)} = (E_v - E_2)/\hbar - \omega_{L_1}. \tag{2}$$

For this hybrid atom-molecular system of N bosons with atomic mass m the energy functional can be written as

$$\begin{aligned} E[n_a,n_m] = \int d\vec{r} \Bigg[& \frac{\hbar^2}{2m}|\vec{\nabla}\sqrt{n_a(\vec{r})}|^2 + U_a(\vec{r})n_a(\vec{r}) \\ & + \xi(n_a)n_a(\vec{r}) + \frac{\hbar^2}{4m}|\vec{\nabla}\sqrt{n_m(\vec{r})}|^2 \\ & + U_m(\vec{r})n_m(\vec{r}) + \frac{\lambda_m}{2}n_m^2(\vec{r}) + \lambda_{am}n_a(\vec{r})n_m(\vec{r}) \\ & + \epsilon n_m(\vec{r}) + \chi n_a(\vec{r})\sqrt{n_m(\vec{r})} \Bigg], \end{aligned} \tag{3}$$

where the perturbative expansion of $\xi(n_a)$ in terms of $n_a a^3$ is given as

$$\xi(n_a) = \frac{\lambda_a}{2}n_a\left[1 + \frac{128}{15\sqrt{\pi}}(n_a a^3)^{1/2}\right], \tag{4}$$

where $n_a(\vec{r})$ and $n_m(\vec{r})$ are the atomic and molecular densities of the system, respectively. $\lambda_a = 4\pi\hbar^2 a/m$; a is the s-wave scattering length for atom-atom interactions. The first term in the above expansion [Eq. (4)] represents the energy of Bose gas within mean-field GP theory calculated by Bogoliubov [33]. The second term was obtained by Lee, Huang, Yang (LHY) [34] using a hard sphere model for interatomic potential. λ_a, λ_m, and λ_{am} represent the strengths of atom-atom, molecule-molecule, and atom-molecule interactions, respectively. We assume here $\lambda_m = \lambda_{am} = \lambda_a$ [8]. The LHY correction term to the Bogoliubov mean-field prediction has been considered only in atom-atom interaction strength but not in the atom-molecule and molecule-molecule interactions. This is an approximation and it is expected that it can be applied when the percentage of molecular formation is not so large. However, to get the exact energy functional, including the higher-order nonlinear term in the atom-molecule and

molecule-molecule interactions, a more sophisticated many-body theory is required. ϵ is a parameter to characterize the effective Raman detuning for a two-photon resonance such that $\epsilon = -\hbar(\delta + \beta_2 - 2\beta_1) = -\hbar\delta_1$. δ_1 is the effective Raman deuning and β_1 and β_2 are atomic and molecular light shift terms which are given as

$$\beta_1 = \sum_{i=1,2} \frac{\left(\Omega_i^A\right)^2}{4D_i} \tag{5}$$

and

$$\beta_2 = \sum_v \left[\frac{(\Omega_2)^2}{4\Delta_v} + \frac{(\Omega_1)^2}{4\Delta_v^{(2)}}\right] |I_{2,v}|^2, \tag{6}$$

where $D_i = \omega_0 - \omega_i$ are the detunings of lasers from the resonance frequency ω_0 of the atomic transition between the dissociation limits of the ground and excited potentials. Ω_1^A and Ω_2^A are the atomic Rabi frequencies for two lasers. $U_a(\vec{r})$ and $U_m(\vec{r})$ are the external trapping potentials for atoms and molecules characterized by two angular frequencies $\omega_\perp$ and ω_z:

$$U_a(\vec{r}) = \tfrac{1}{2}m\omega_\perp^2\left(x^2 + y^2 + \lambda_0^2 z^2\right) \tag{7}$$

and

$$U_m(\vec{r}) = m\omega_\perp^2\left(x^2 + y^2 + \lambda_0^2 z^2\right), \tag{8}$$

where $\lambda_0 = \omega_z/\omega_\perp$ is the anisotropy parameter ($\lambda_0 = 1$ corresponds to spherically symmetric trap). As we neglect particle loss, the total number of particles is a conserved quantity.

$$\int n(\vec{r})d\vec{r} = \int [n_a(\vec{r}) + 2n_m(\vec{r})]\, d\vec{r} = \int [|\psi_a(\vec{r})|^2 + 2|\psi_m(\vec{r})|^2]\, d\vec{r} = N, \tag{9}$$

where $n(\vec{r})$ is the total density of the system and $\psi_a(\vec{r})$ and $\psi_m(\vec{r})$ are the atomic and molecular condensate wave functions, respectively. By performing the functional variation with Lagrange multiplier μ one finds the Euler-Lagrange equations as $\delta(E - \mu N)/\delta\psi_a^*(\vec{r}) = 0$ and $\delta(E - \mu N)/\delta\psi_m^*(\vec{r}) = 0$. These equations take on the form of coupled time-independent versions of the modified GP (MGP) equations,

$$\mu\psi_a = \left[-\frac{\hbar^2\nabla^2}{2m} + U_a(\vec{r}) + \lambda_a\left(1 + \frac{32a^{3/2}}{3\pi^{1/2}}\psi_a\right)\psi_a^2 + \lambda_{am}\psi_m^2\right]\psi_a + \chi\psi_m\psi_a \tag{10}$$

$$2\mu\psi_m = \left[-\frac{\hbar^2\nabla^2}{4m} + U_m(\vec{r}) + \epsilon + \lambda_m\psi_m^2 + \lambda_{am}\psi_a^2\right]\psi_m + \frac{\chi}{2}\psi_a^2. \tag{11}$$

In Eqs. (10) and (11), μ and 2μ play the role of atomic and molecular chemical potential, respectively. If the LHY term is neglected in Eq. (10) the equation for ψ_a reduces to the GP equation as follows,

$$\mu_a\psi_a = \left[-\frac{\hbar^2\nabla^2}{2m} + U_a(\vec{r}) + \lambda_a\psi_a^2 + \lambda_{am}\psi_m^2\right]\psi_a + \chi\psi_m\psi_a \tag{12}$$

Here the atom-atom scattering length (a) depends on the laser intensities [6] in the following manner:

$$a = a_{bg} - \frac{m}{4\pi\hbar}\sum_v \left[\frac{\Omega_1^2}{4\Delta_v} + \frac{\Omega_2^2}{4\Delta_v^{(1)}}\right]\left|I_{1,v}^2\right|, \tag{13}$$

where a_{bg} is the background scattering length.

The stationary states of the hybrid atom-molecular system can be obtained using the MGP approach [by solving coupled Eqs. (10) and (11)] and using the GP approach [by solving Eqs. (11) and (12)]. These time-independent coupled nonlinear Schrödinger equations have been solved numerically by means of imaginary time propagation method to give the stable solutions. The details of the numerical method have been discussed elsewhere [24]. We will show here that the effect of LHY correction term to the mean-field atom-atom interaction on the static properties and the collective excitation frequencies of the hybrid system becomes important when the peak gas-parameter of this hybrid system is large, i.e., $x_{pk} \geqslant 10^{-3}$.

The total energy per particle of the system can be written as

$$\frac{E}{N} = T_a + T_m + U_a + U_m + E_{aa_1} + E_{aa_2} + E_{mm} + E_{am} + E_d + E_c. \tag{14}$$

The kinetic energies per particle for atoms (T_a) and molecules (T_m) are given by

$$T_a = T_{\perp,a} + T_{z,a} = \frac{1}{N}\left[\frac{\hbar^2}{2m}\int d\vec{r}|\partial_r\psi_a(\vec{r})|^2 + \frac{\hbar^2}{2m}\int d\vec{r}|\partial_z\psi_a(\vec{r})|^2\right], \tag{15a}$$

$$T_m = T_{\perp,m} + T_{z,m} = \frac{1}{N}\left[\frac{\hbar^2}{4m}\int d\vec{r}|\partial_r\psi_m(\vec{r})|^2 + \frac{\hbar^2}{4m}\int d\vec{r}|\partial_z\psi_m(\vec{r})|^2\right]. \tag{15b}$$

Here $T_{\perp,a}$ and $T_{\perp,m}$ ($T_{z,a}$ and $T_{z,m}$) are the transverse components (z components) of kinetic energy of atoms and molecules, respectively.

The trapping potential energies per particle for atoms (U_a) and molecules (U_m) are described by

$$U_a = U_{\perp,a} + U_{z,a} = \frac{1}{N}\left[\frac{1}{2}m\omega_\perp^2\int d\vec{r}(x^2 + y^2)|\psi_a(\vec{r})|^2 + \frac{1}{2}m\lambda_0^2\omega_\perp^2\int d\vec{r}z^2|\psi_a(\vec{r})|^2\right], \tag{16a}$$

$$U_m = U_{\perp,m} + U_{z,m} = \frac{1}{N}\left[m\omega_\perp^2\int d\vec{r}(x^2 + y^2)|\psi_m(\vec{r})|^2 + m\lambda_0^2\omega_\perp^2\int d\vec{r}z^2|\psi_m(\vec{r})|^2\right]. \tag{16b}$$

Here $U_{\perp,a}$ and $U_{\perp,m}$ ($U_{z,a}$ and $U_{z,m}$) are the transverse components (z components) of trap energy of atoms and molecules, respectively.

E_{aa_1}, E_{aa_2}, E_{mm}, and E_{am} are the energies per particle for the atom-atom (in mean-field GP theory), atom-atom (due

to the LHY term), molecule-molecule, and atom-molecule interactions, respectively, and are given as

$$E_{aa_1} = \frac{\lambda_a}{2N}\int d\vec{r}|\psi_a(\vec{r})|^4, \tag{17a}$$

$$E_{aa_2} = \frac{\lambda_a}{2N}\left(\frac{128}{15}\right)\left(\frac{a^3}{\pi}\right)^{1/2}\int d\vec{r}|\psi_a(\vec{r})|^5, \tag{17b}$$

$$E_{mm} = \frac{\lambda_m}{2N}\int d\vec{r}|\psi_m(\vec{r})|^4, \tag{17c}$$

$$E_{am} = \frac{\lambda_{am}}{N}\int d\vec{r}|\psi_a(\vec{r})|^2|\psi_m(\vec{r})|^2. \tag{17d}$$

The energy per particle due to the effective Raman detuning (E_d) and the coupling (E_c) between atoms and molecules are given by

$$E_d = \frac{\epsilon}{N}\int d\vec{r}|\psi_m(\vec{r})|^2, \tag{18}$$

$$E_c = \frac{\chi}{N}\int d\vec{r}|\psi_a(\vec{r})|^2\psi_m(\vec{r}), \tag{19}$$

where $\lambda_0 = 1$ corresponds to the case of spherically symmetric trap.

The virial relation that must be satisfied by the energy components is

$$2[T_a + T_m] - 2[U_a + U_m] + 3[E_{aa_1} + E_{mm} + E_{am}] + \tfrac{9}{2}E_{aa_2} + \tfrac{3}{2}E_c = 0. \tag{20}$$

B. Collective excitations: sum-rule approach

According to the sum-rule approach [27,28], the upper bound of the lowest excitation energy is given by

$$\hbar\Omega = \sqrt{\frac{m_3}{m_1}}, \tag{21}$$

where $m_p = \sum_n |\langle 0|F|n\rangle|^2(\hbar\Omega_{n0})$ is the pth order moment of excitation energy and F is the general excitation operator for low-energy excitations of many-body states. Ω is the frequency of excitation and $\hbar\Omega_{n0} = E_n - E_0$ is the excitation energy of the eigenstate $|n\rangle$ of the hybrid atom-molecular system. The moments m_1 and m_3 can be expressed as the expectation values of the commutators between F and Hamiltonian H with respect to the ground state ($|0\rangle$) as [27,28]

$$m_1 = \tfrac{1}{2}\langle 0|[F^\dagger,[H,F]]|0\rangle, \tag{22}$$

$$m_3 = \tfrac{1}{2}\langle 0|[[F^\dagger,H],[H,[H,F]]]|0\rangle. \tag{23}$$

Here we are considering the collective modes characterized by the z component of the angular-momentum index $m' = 2$ and $m' = 0$ which have been experimentally studied on atomic BEC [10,11]. The collective mode $m' = 2$ describes the case in which the hybrid system expands in one direction and simultaneously contracts in the other, maintaining its volume. The $m' = 0$ mode describes the situation in which the system alternatively expands and contracts in the radial direction. The system also experiences oscillations in the axial direction out of phase with the radial motion due to the repulsive interaction.

Following Kimura *et al.* [30] the excitation operators to $m' = 2$ and $m' = 0$ mode can be given as

$$F_{m'=2} = \sum_i \left(x_i^2 - y_i^2\right), \tag{24}$$

$$F_{m'=0} = \sum_i \left(x_i^2 + y_i^2 - \gamma z_i^2\right), \tag{25}$$

where γ is a variational parameter characterizing the coupling of monopole and quadrupole modes for the axially symmetric trap. The value of the parameter γ can be obtained by making the excitation energy Ω extremum. For spherically symmetric trap the two modes get decoupled.

Using the energy functional given by Eq. (3) together with the Eq. (4) and performing some tedious algebra the expressions for the moments m_1 and m_3 can be obtained for the $m' = 2$ and $m' = 0$ modes of excitations. For the $m' = 2$ mode and in the case of the axially symmetric trap the first and the third moments are obtained as

$$m_1 = \frac{\hbar^2}{m^2}\left[4\frac{U_{\perp,a}}{\omega_\perp^2} + \frac{U_{\perp,m}}{\omega_\perp^2}\right], \tag{26}$$

$$m_3 = 2\frac{\hbar^4}{m^2}[4(T_{\perp,a} + U_{\perp,a}) + (T_{\perp,m} + U_{\perp,m})]. \tag{27}$$

By substituting Eqs. (26) and (27) in (21) we get the following:

$$\frac{\Omega_{m'=2}^2}{\omega_\perp^2} = 2\left[\frac{4(T_{\perp,a} + U_{\perp,a}) + (T_{\perp,m} + U_{\perp,m})}{4U_{\perp,a} + U_{\perp,m}}\right]. \tag{28}$$

For a spherically symmetric trap $\lambda_0 = 1, \omega_\perp = \omega_z = \omega_{HO}$ and the excitation frequency can be written as

$$\frac{\Omega_{m'=2}^2}{\omega_{HO}^2} = 2\left[\frac{4(T_a + U_a) + (T_m + U_m)}{4U_a + U_m}\right]. \tag{29}$$

The frequency of $m' = 2$ mode is not affected by the interaction and coupling energies.

For $m' = 0$ mode and axially symmetric trap, we obtain the first moment m_1 as

$$m_1 = \frac{4\hbar^2}{m^2}\left[\frac{U_{\perp,a}}{\omega_\perp^2} + \gamma^2\frac{U_{z,a}}{\omega_z^2}\right] + \frac{\hbar^2}{m^2}\left[\frac{U_{\perp,m}}{\omega_\perp^2} + \gamma^2\frac{U_{z,m}}{\omega_z^2}\right] \tag{30}$$

and the third moment m_3 as

$$m_3 = \frac{8\hbar^4}{m^2}\left[(T_{\perp,a} + \gamma^2 T_{z,a}) + (U_{\perp,a} + \gamma^2 U_{z,a}) + (1 - \gamma/2)^2 \times \left(E_{aa_1} + \frac{9}{4}E_{aa_2} + E_{am} + \frac{1}{4}E_c\right)\right] + \frac{2\hbar^4}{m^2}[(T_{\perp,m} + \gamma^2 T_{z,m}) + (U_{\perp,m} + \gamma^2 U_{z,m}) + (1 - \gamma/2)^2(E_{mm} + E_{am})] \tag{31}$$

and hence from Eq. (21)

$$\Omega_{m'=0}^2 = \left\{8\left[(T_{\perp,a} + \gamma^2 T_{z,a}) + (U_{\perp,a} + \gamma^2 U_{z,a}) + (1 - \gamma/2)^2\left(E_{aa_1} + \frac{9}{4}E_{aa_2} + E_{am} + \frac{1}{4}E_c\right)\right]\right.$$

$$+2[(T_{\perp,m}+\gamma^2 T_{z,m})+(U_{\perp,m}+\gamma^2 U_{z,m}) + (1-\gamma/2)^2(E_{mm}+E_{am})]\Big\}\Big/ \left\{4\left[\frac{U_{\perp,a}}{\omega_\perp^2}+\gamma^2\frac{U_{z,a}}{\omega_z^2}\right]+\left[\frac{U_{\perp,m}}{\omega_\perp^2}+\gamma^2\frac{U_{z,m}}{\omega_z^2}\right]\right\}. \quad (32)$$

Minimization of $\Omega^2_{m'=0}$ with respect to γ leads to a quadratic equation in γ. The two roots ($\gamma_\pm$) of this equation correspond to the maximum and minimum values of $\Omega^2_{m'=0}$.

In the case of a spherically symmetric trap ($\lambda_0 = 1$) the two roots of γ are 2 and -1, corresponding to the quadrupole and monopole modes, respectively. The frequency corresponding to $\gamma = 2$ is

$$\frac{\Omega^2_{m'=0}}{\omega^2_{HO}} = 2\left[\frac{4(T_a+U_a)+(T_m+U_m)}{4U_a+U_m}\right] \quad (33)$$

and the frequency corresponding to $\gamma = -1$ is

$$\frac{\Omega^2_{m'=0}}{\omega^2_{HO}} = \left\{8\left[T_a+U_a+\frac{9}{4}\left(E_{aa_1}+\frac{9}{4}E_{aa_2}+E_{am}+\frac{1}{4}E_c\right)\right] +2\left[T_m+U_m+\frac{9}{4}(E_{mm}+E_{am})\right]\right\}\Big/(4U_a+U_m). \quad (34)$$

It is evident from Eqs. (29) and (33) that, in the case of spherically symmetric trap expressions for the $\Omega_{m'=2}$ mode and $\Omega_{m'=0}$ ($\gamma = 2$) are identical and they are independent of atom-atom, molecule-molecule, and atom-molecule interaction energies and atom-molecule coupling energy. If the calculation is restricted within the mean-field GP approximation only, then $E_{aa_2} = 0$. We have investigated the variation of the collective excitation frequencies of an atom-molecular hybrid system with the effective Raman detuning, the *s*-wave scattering length, and the laser intensities. In this work we have compared the collective excitation frequencies of the hybrid atom-molecular condensates with those for a pure atomic BEC. The excitation frequency for $m' = 0$ ($\gamma = -1$) mode of a spherically trapped and for $m' = 0$ ($\gamma+$) mode for an axially trapped atomic BEC can be obtained from the Eqs. (28) and (29) in Ref. [24].

III. RESULTS AND DISCUSSIONS

In this calculation we have considered the atoms and molecules of ^{87}Rb to study the stationary state of the hybrid atomic-molecular condensate system. The *s*-wave scattering length for the rubidium atom in the absence of the light field is a_{bg}= 100 a_0 [35,36]. We have considered Raman photoassociation for the formation of molecular condensate in the ground $^3\Sigma_u^+$ state ($V_g(R)$) via 0_g^- excited state ($V_e(R)$) of $^{87}Rb_2$ molecule and have chosen the parameters characterizing the coupled system as $\Omega_1 = 2\times10^{10}$ s^{-1},$\Omega_2 = 6.324\times10^9$ s^{-1}, $\chi/\hbar = 7.6\times10^{-7}$ m$^{3/2}$ s^{-1},$\beta_1 = 2.108\times10^7$ s^{-1},$\beta_2 = 3.344\times10^6$ s^{-1},$\delta = 3.879\times10^7$ s^{-1},$\delta_1 = 2.8\times10^4$ s^{-1} and the laser-induced modified scattering length $a = 5.4$ nm as given in our previous study [8]. Here the laser intensities I_1 and I_2 are 159.2 and 79.6 W/cm^2, respectively. For this calculation we have considered the value of $N = 5\times10^5$, the spherical trap with frequency $\omega_{HO} = 2\pi\times100$ Hz [6,8], and the axial trap with $\omega_\perp = 2\pi\times54$ Hz and $\omega_z = 2\pi\times153$ Hz [1].

TABLE I. Comparison between GP and MGP results for the ground-state properties of coupled condensate system containing 5×10^5 ^{87}Rb atoms in a spherical trap with $\frac{\omega_{HO}}{2\pi} = 100$ Hz. δ_1 is kept fixed at 8×10^4 s^{-1}. $\chi/\hbar = 7.6\times10^{-7}$ m$^{3/2}$ s^{-1}. Total energy per particle (E/N), chemical potential for atomic condensate (μ_a), and the peak gas parameter (x_{pk}) for different values of a are given. The chemical potential for molecular condensate $\mu_m = 2\mu_a$. E/N and μ_a are in the units of $\hbar\omega_{HO}$.

a (nm)		μ_a	E/N	x_{pk}
5.4	GP	32.59	23.37	7.29(−5)
	MGP	33.09	23.69	7.04(−5)
8	GP	38.55	27.63	1.84(−4)
	MGP	39.46	28.20	1.74(−4)
15	GP	50.10	35.87	8.16(−4)
	MGP	52.44	37.36	7.38(−4)
25	GP	61.76	44.20	2.76(−3)
	MGP	66.70	47.37	2.36(−3)

First, we have presented the results for ground-state properties (chemical potential, total energy per particle, and peak gas parameter) and then the results for collective excitations of hybrid atomic-molecular condensate of ^{87}Rb. The dependence of ground-state properties on the *s*-wave scattering length has been studied and the results have been given in Tables I and II for spherically and axially trapped ^{87}Rb Bose condensates, respectively. The variation of the *s*-wave scattering length is experimentally feasible by optically induced Feshbach resonance using one photon scheme and by using an optical Feshbach resonance with a two-photon Raman transition in a BEC of ^{87}Rb [35,36]. The effective Raman detuning δ_1 is kept fixed at 8×10^4 s^{-1}. The parameter δ_1 can be adjusted by

TABLE II. Comparison between GP and MGP results for the ground-state properties of coupled condensate system containing 5×10^5 ^{87}Rb atoms in an axial trap with $\frac{\omega_\perp}{2\pi} = 54$ Hz and $\frac{\omega_z}{2\pi} = 153$ Hz. δ_1 is kept fixed at 8×10^4 s^{-1}. $\chi/\hbar = 7.6\times10^{-7}$ m$^{3/2}$ s^{-1}. Total energy per particle (E/N), chemical potential for atomic condensate (μ_a), and the peak gas parameter (x_{pk}) for different values of a are given. The chemical potential for molecular condensate $\mu_m = 2\mu_a$. E/N and μ_a are in the units of $\hbar\omega_\perp$.

a (nm)		μ_a	E/N	x_{pk}
5.4	GP	43.78	31.18	5.16(−5)
	MGP	44.35	31.54	5.01(−5)
8	GP	51.72	36.85	1.32(−4)
	MGP	52.77	37.52	1.26(−4)
15	GP	67.17	47.86	5.83(−4)
	MGP	69.91	49.58	5.15(−4)
25	GP	82.75	59.09	2.05(−3)
	MGP	88.80	62.74	1.90(−3)

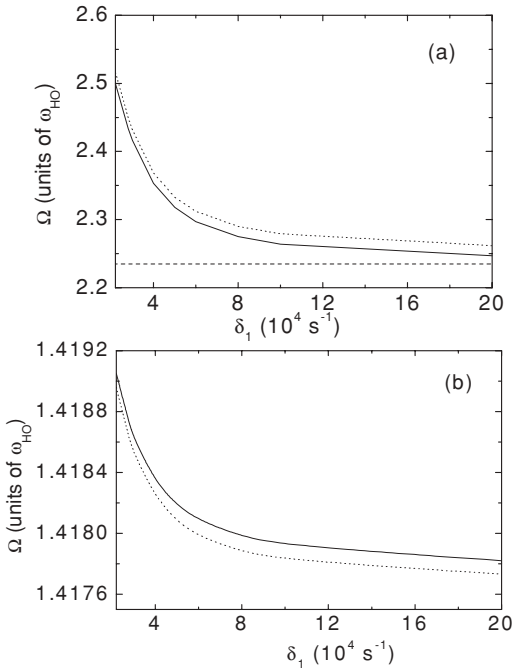

FIG. 2. The collective oscillation frequencies of the hybrid atom-molecular system confined in a spherically symmetric trap as functions of effective Raman detuning δ_1. $\omega_{HO} = 2\pi \times 100$ Hz and $a = 5.4$ nm. $\chi/\hbar = 7.6 \times 10^{-7}$ m$^{3/2}$ s^{-1}. The solid and dotted lines represent the GP and MGP results for (a) $m' = 0$ ($\gamma = -1$) [Eq. (34)] and (b) $m' = 0$ ($\gamma = 2$) (equivalent to $m' = 2$) [Eqs. (29) and (33)] modes. For comparison the GP excitation frequency for $m' = 0$ ($\gamma = -1$) mode of a pure atomic BEC is indicated by the horizontal dashed line in Fig. 2(a) (see text).

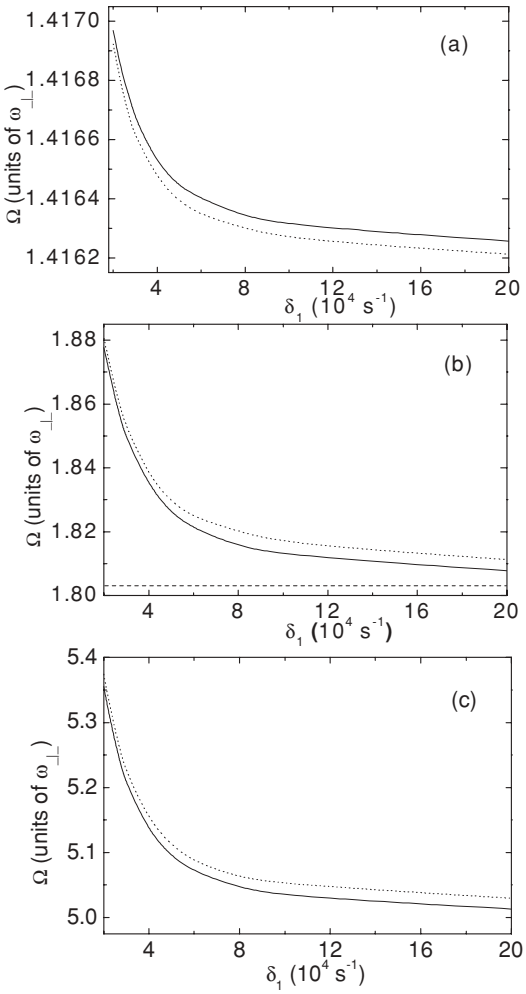

FIG. 3. The collective excitation frequencies of the hybrid atom-molecular system confined in an axially symmetric trap as functions of effective Raman detuning δ_1. $\omega_\perp = 2\pi \times 54$ Hz and $\omega_z = 2\pi \times 153$ Hz. $a = 5.4$ nm and $\chi/\hbar = 7.6 \times 10^{-7}$ m$^{3/2}$ s^{-1}. The solid and dotted lines represent the GP and MGP results for (a) $m' = 2$ [Eq. (28)], [(b) $m' = 0$ ($\gamma+$) and (c) $m' = 0$ ($\gamma-$)] [Eq. (32)] modes. For comparison the GP excitation frequency for $m' = 0$ ($\gamma+$) mode of a pure atomic BEC is indicated by the horizontal dashed line in Fig. 3(b) (see text).

tuning the value of ω_{L_2} and keeping ω_{L_1} fixed. It is found that for both the traps chemical potentials and the total energy per particle from GP and MGP approaches are very close to each other for small values of s-wave scattering length a. But the difference in GP and MGP results becomes significant for large values of a, i.e., for $x_{pk} \sim 10^{-3}$ or more. For these calculations the virial relation is satisfied within the limit $\leqslant 8 \times 10^{-5}$.

The results for the frequencies of collective excitations of the hybrid atomic-molecular condensates for the modes $m' = 2$ and $m' = 0$ as a function of δ_1 have been shown in Figs. 2 and 3 for spherically and axially symmetric traps, respectively. In both the cases a remains constant at 5.4 nm. Figures 2(a) and 2(b) present the excitation frequencies for $m' = 0$ ($\gamma = -1$) and $m' = 0$ ($\gamma = 2$) mode, respectively. The dotted lines represent results for the MGP approach while the corresponding GP results are shown by the solid lines. Figure 2(b) also gives the values for $m' = 2$ mode which are equal to the values for $m' = 0$ ($\gamma = 2$) mode as given by Eqs. (29) and (33). In Fig. 3 solid and dotted lines represent GP and MGP results for the excitation frequencies for axially symmetric trap as a function of δ_1 for $m' = 2$ [Fig. 3(a)], $m' = 0$ ($\gamma+$) [Fig. 3(b)] and $m' = 0$ ($\gamma-$) [Fig. 3(c)] modes, respectively. It is evident from Figs. 2 and 3 that at smaller values of δ_1 GP and MGP excitation frequencies almost coincide but the difference increases with the increase in the values of δ_1 and becomes almost constant after $\delta_1 = 6 \times 10^4$ s^{-1}. The excitation frequencies for $m' = 0$ ($\gamma = -1$) mode in case of spherical trap and $m' = 0$ ($\gamma_\pm$) modes in case of axially symmetric trap are functions of interaction energies which include the energy due to LHY interactions (E_{aa_2}). This leads to the difference in the excitation frequencies for GP and MGP approaches. Since in this case the s-wave scattering length is 5.4 nm, the difference is not so large [Figs. 2(a), 3(b), and 3(c)]. However, the excitation frequencies for $m' = 2$ (equivalent to $m' = 0$; $\gamma = 2$) mode in case of spherical trap and $m' = 2$ mode in case of axial trap are independent of the interaction energies but depend on the trap potential, kinetic energy, and the static density of atoms and molecules. In this case, small difference in the excitation frequencies from GP and MGP approaches arises because of the difference in the static densities of atoms and molecules obtained from GP and MGP calculations [note the change in scale form Figs. 2(a) to 2(b) and from Figs. 3(a) to 3(b) and Figs. 3(a) to 3(c)].

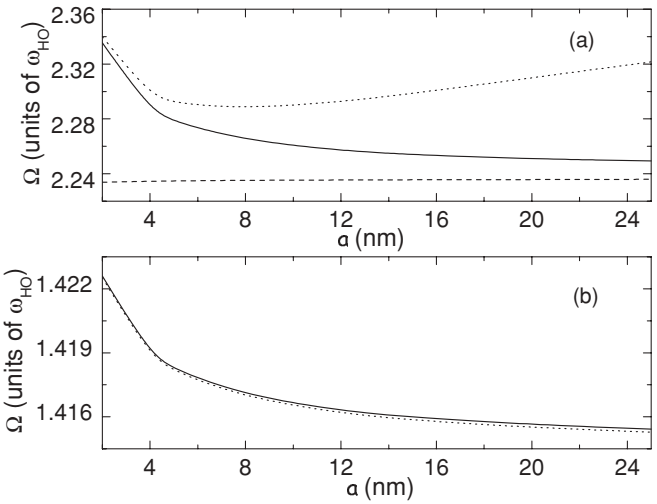

FIG. 4. The collective excitation frequencies of the hybrid atom-molecular system confined in a spherically symmetric trap as functions of s-wave scattering length a. $\omega_{HO} = 2\pi \times 100$ Hz, $\delta_1 = 8 \times 10^4$ s^{-1} and $\chi/\hbar = 7.6 \times 10^{-7}$ m$^{3/2}$ s^{-1}. The solid and dotted lines represent the GP and MGP results for (a) $m' = 0$ ($\gamma = -1$) [Eq. (34)] and (b) $m' = 0$ ($\gamma = 2$) (equivalent to $m' = 2$) [Eqs. (29) and (33)] modes. The dashed line in Fig. 4(a) represents the GP excitation frequency for $m' = 0$ ($\gamma = -1$) mode of a pure atomic BEC as a function of a (see text).

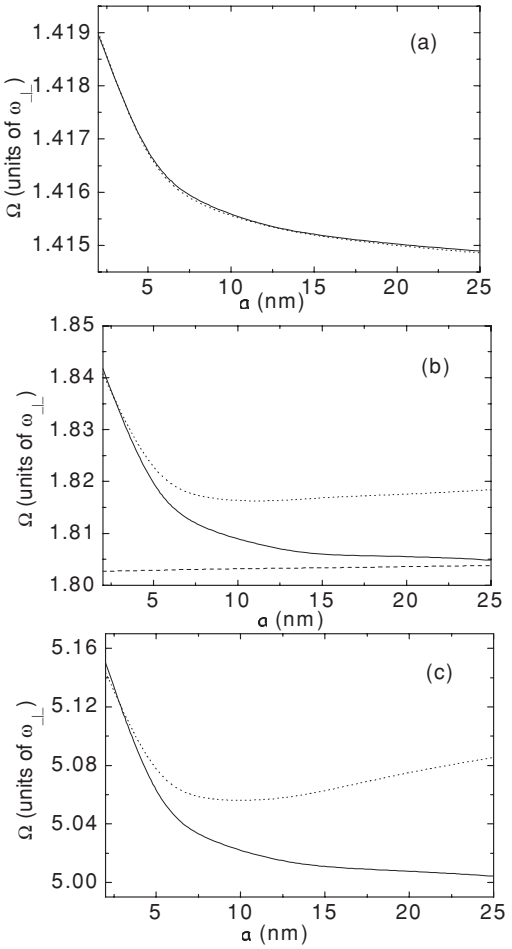

FIG. 5. The collective excitation frequencies of the hybrid atom-molecular system confined in an axially symmetric trap as functions of a. $\omega_\perp = 2\pi \times 54$ Hz and $\omega_z = 2\pi \times 153$ Hz. $\delta_1 = 8 \times 10^4$ s^{-1} and $\chi/\hbar = 7.6 \times 10^{-7}$ m$^{3/2}$ s^{-1}. The solid and dotted lines represent the GP and MGP results for (a) $m' = 2$ [Eq. (28)], [(b) $m' = 0$ ($\gamma+$) and (c) $m' = 0$ ($\gamma-$)] [Eq. (32)] modes. The dashed line in Fig. 5(b) represents the GP excitation frequency for $m' = 0$ ($\gamma+$) mode of a pure atomic BEC as a function of a (see text).

In order to compare the results of the excitation frequencies for the hybrid atom-molecular system with those for a pure atomic BEC we have calculated the GP values of $m' = 0$ ($\gamma = -1$) mode for the spherically trapped and $m' = 0$ ($\gamma+$) mode for the axially trapped ^{87}Rb atomic condensate with 5×10^5 atoms and $a = 5.4$ nm. The values of these two modes are found to be 2.235 (in the unit of ω_{HO}) and 1.803 (in the unit of $\omega_\perp$), respectively. These have been shown as the horizontal dashed lines in Figs. 2(a) and 3(b) for comparison. It is to be mentioned here that the excitation frequencies for an atomic BEC are independent of δ_1. Figures 2(a) and 3(b) clearly show that the excitation frequencies for the hybrid atom-molecular condensates approaches the excitation frequencies for a pure atomic BEC as detuning becomes larger and atom-to-molecule conversion efficiency (η) is reduced. The value of η is 19% at $\delta_1 = 2.8 \times 10^4$ s^{-1}, whereas it reduces to 0.4% at $\delta_1 = 2 \times 10^5$ s^{-1} for the spherically trapped hybrid condensate. Similarly the values of η are 13% and 0.2% at $\delta_1 = 2.8 \times 10^4$ s^{-1} and 2×10^5 s^{-1}, respectively, for the axially trapped atom-molecular coupled system.

In Figs. 4(a) and 4(b) we show the behavior of the $m' = 0$ ($\gamma = -1$) mode and $m' = 0$ ($\gamma = 2$) (equivalent to $m' = 2$ mode) mode frequencies as a function of a for the spherically trapped system. The effective Raman detuning δ_1 is kept fixed at 8×10^4 s^{-1}. Solid and dotted lines represent GP and MGP results. It is found from Eq. (34) that the excitation frequency for the $m' = 0$ ($\gamma = -1$) mode is a function of all the interaction energies. The interaction energies for atom-atom, atom-molecule, molecule-molecule, and higher-order LHY interactions strongly depend on s-wave scattering length (a). It is known that the effect of the higher-order LHY term increases with the increase in a and hence the signature of higher-order nonlinear effect will be prominent on the excitation frequencies for the $m' = 0$ ($\gamma = -1$) mode with the increase in a. This feature is evident in Fig. 4(a), where the GP and MGP excitation frequencies for the $m' = 0$ ($\gamma = -1$) mode initially decrease as a increases, but after $a = 4$ nm the MGP excitation frequency deviates significantly from the GP frequency and increases with the increase in a. Whereas excitation frequency for the $m' = 0$ ($\gamma = 2$) mode depends only on the kinetic energy and the trapping potential [see Eq. (33)], the small difference between the GP and MGP excitation frequencies for the $m' = 0$ ($\gamma = 2$) mode arises due to the difference in the static densities n_a and n_m obtained from GP and MGP approaches [see Fig. 4(b)]. Figures 5(a), 5(b), and 5(c) demonstrate the excitation frequencies for the $m' = 2$, $m' = 0$ ($\gamma+$), and $m' = 0$ ($\gamma-$) modes, respectively, as a function of a for axial trap. As in the case of spherical trap, the difference between GP and MGP results enhances for the large values of a for $m' = 0$ ($\gamma_\pm$) mode but for $m' = 2$ mode the GP and MGP results almost coincide in case of axially

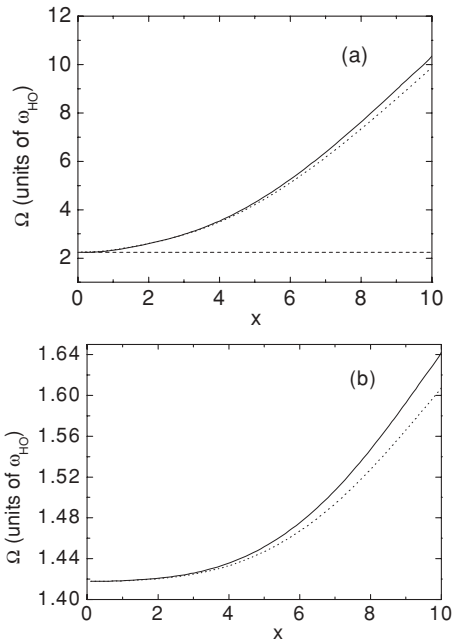

FIG. 6. The collective excitation frequencies of the hybrid atom-molecular system confined in a spherically symmetric trap as functions of the parameter x. $\omega_{HO} = 2\pi \times 100$ Hz. The solid and dotted lines represent the GP and MGP results for (a) $m' = 0$ ($\gamma = -1$) [Eq. (34)] and (b) $m' = 0$ ($\gamma = 2$) (equivalent to $m' = 2$) [Eqs. (29) and (33)] modes. For comparison the GP excitation frequency for $m' = 0$ ($\gamma = -1$) mode of a pure atomic BEC is indicated by the horizontal dashed line in Fig. 6(a) (see text).

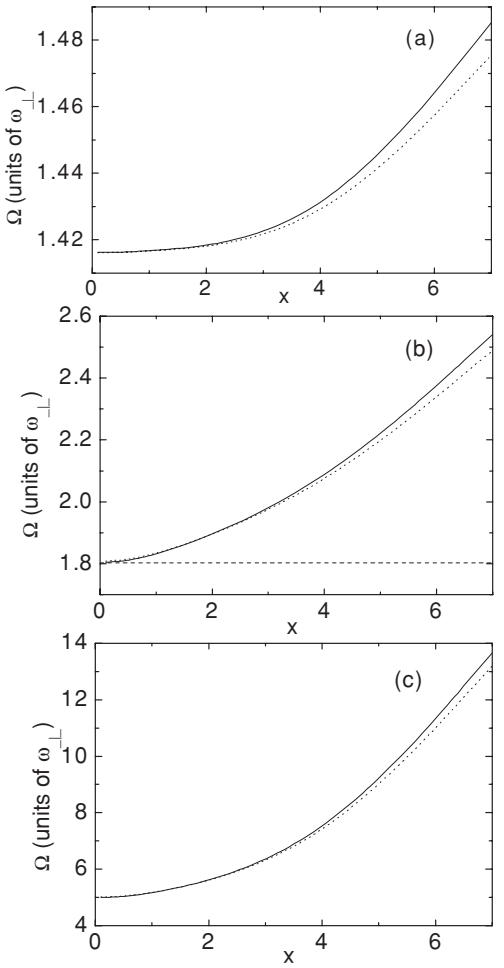

FIG. 7. The collective excitation frequencies of the hybrid atom-molecular system confined in an axially symmetric trap as functions of the parameter x. $\omega_\perp = 2\pi \times 54$ Hz and $\omega_z = 2\pi \times 153$ Hz. The solid and dotted lines represent the GP and MGP results for (a) $m' = 2$ [Eq. (28)], [(b) $m' = 0$ ($\gamma+$) and (c) $m' = 0$ ($\gamma-$)] [Eq. (32)] modes. For comparison the GP excitation frequency for $m' = 0$ ($\gamma+$) mode of a pure atomic BEC is indicated by the horizontal dashed line in Fig. 7(b) (see text).

trapped system. This feature arises as the interaction energies contribute only in the $m' = 0$ mode excitation frequency [Eq. (32)] and does not contribute in the $m' = 2$ mode excitation [Eq. (28)].

We also attempt to compare here the $m' = 0$ ($\gamma = -1$) mode frequency for the spherically trapped hybrid system and $m' = 0$ ($\gamma+$) mode frequency for the cylindrically trapped hybrid condensate with the respective modes obtained for a pure atomic BEC. In Figs. 4(a) and 5(b) the GP excitation frequencies for $m' = 0$ ($\gamma = -1$) and $m' = 0$ ($\gamma+$) modes of an atomic condensate are plotted (dashed line) as a function of a in the cases of spherically and axially symmetric traps, respectively. It can be seen that for both the traps the two results differ moderately for the smaller values of a as the value of η is higher for smaller a. The deviations of the excitation frequencies of the hybrid system from those of the atomic BEC are 5% and 2.2% for $a = 2$ nm in case of spherical and axial traps, respectively. The GP values of atom-to-molecule conversion efficiency (η) are 5.3% and 2% for $a = 2$ nm and 25 nm, respectively, in case of spherical trap. Similarly the GP values of η are 4% and 1.4% for $a = 2$ nm and 25 nm, respectively in the case of an axial trap.

To show how the excitation frequencies of the hybrid system depends on the atom-molecule coupling strength (χ) we have changed the intensities of both lasers by a factor x, keeping the intensity ratio I_2/I_1 constant. Consequently, for the new set of intensities the Rabi frequencies (Ω_1 and Ω_2) change and hence the magnitude of atom-molecule coupling strength (χ) also changes [see Eq. (1)]. The other relevant parameter, e.g., atomic s-wave scattering length (a) are modified accordingly [see Eq. (13)]. For $x = 1$ and 10, a becomes 5.4 and 6.37 nm, respectively. The value of effective two-photon Raman detuning is kept constant at $\delta_1 = 8 \times 10^4$ s^{-1}. In order to keep the parameter δ_1 constant for different values of intensities we need to change the value of two-photon Raman detuning (δ) accordingly, e.g., δ assumes the value 0.38×10^7 s^{-1} for $x = 0.1$ and 38.81×10^7 s^{-1} for $x = 10$ to keep δ_1 fixed at 8×10^4 s^{-1}. Figures 6 and 7 show how the low-energy excitation frequencies increase with the parameter x in the case of spherically and axially symmetric traps, respectively. The dependence of excitation frequencies on x for the $m' = 0$ ($\gamma = -1$) and $m' = 0$ ($\gamma = 2$) modes are shown in Figs. 6(a) and 6(b), respectively. The $m' = 2$ mode is equivalent to the $m' = 0$ ($\gamma = 2$) mode in the case of a spherical trap. Figures 7(a), 7(b), and 7(c) demonstrate the dependence of excitation frequencies for $m' = 2$, $m' = 0$ ($\gamma+$), and $m' = 0$

($\gamma-$) modes on x for axially trapped system. In both Figs. 6 and 7 the solid and dotted lines correspond to GP and MGP results. As illustrated in these two figures, the excitation frequencies for $m' = 0$ and $m' = 2$ modes increase smoothly with the increase in laser intensities. This feature is due to the enhancement of the atom-molecule coupling strength with the increase in laser intensity. Since the s-wave scattering length increases with laser intensity, the effect of the higher-order nonlinear term (LHY) becomes prominent with the increase in laser intensity. As a result the difference between GP and MGP results widens for the $m' = 0$ ($\gamma = -1$) mode in the case of a spherical trap [Fig. 6(a)] and $m' = 0$ ($\gamma_{\pm}$) in case of axial trap [Figs. 7(b) and 7(c)]. However, the difference is not so large for $m' = 0$ ($\gamma = 2$) in the case of a spherical trap [Fig. 6(b)] and the $m' = 2$ mode in the case of an axial trap [Fig. 7(a)] [note the change in scale from Figs. 6(a) to 6(b), 7(a) to 7(b), and 7(a) to 7(c)]. The small difference between GP and MGP results for these two frequencies results from the difference between static densities n_a and n_m obtained in GP and MGP approaches.

The value of the $m' = 0$ ($\gamma = -1$) mode excitation frequency for a spherically trapped pure atomic BEC of 5×10^5 ^{87}Rb atom is shown by a horizontal dashed line in Fig. 6(a). Similarly, in the case of an axially symmetric trap the $m' = 0$ ($\gamma+$) mode excitation frequency for a pure atomic BEC has been shown by a horizontal dashed line in Fig. 7(b). When the coupling strength χ is small there are no differences between the results for a hybrid atom-molecular condensate and a purely atomic BEC as the atom-to-molecule conversion efficiency is negligible, e.g., η is 0.1% for $x = 0.25$. With the increase in the coupling strength χ (i.e., with the increase in the parameter x) the atom-to-molecule conversion efficiency increases and the results for the hybrid atom-molecular and pure atomic condensate deviate significantly. The excitation frequencies for $x = 7$ for the hybrid atom-molecular system are 2.8 and 1.4 times larger than those for atomic BEC in case of spherical and axial traps, respectively. These deviations of the excitation frequencies for the atom-molecule hybrid system from those for the single atomic BEC can be considered as the signature of atom-to-molecule conversion by Raman photoassociation.

IV. CONCLUSIONS

In this article, we have presented the ground-state properties and collective excitations of a hybrid atomic-molecular condensate and have studied its dependence on the detuning, atom-molecule coupling strength and the scattering length of atom-atom interaction. We have also demonstrated the importance of the higher-order LHY term (in MGP theory) in the interatomic correlation energy obtained from the ground-state energy of a Bose gas as the peak gas-parameter (x_{pk}) becomes $\geqslant 10^{-3}$. We have derived the expressions for frequencies of low-energy excitations in the sum-rule approach, including the higher-order nonlinear term (LHY) both for spherically and axially trapped hybrid condensate systems. The excitation frequencies are functions of atomic and molecular condensate densities and the condensate densities have been obtained by solving the time-independent coupled equations for atomic and molecular BECs of ^{87}Rb using imaginary time method. We have studied the dependence of the excitation frequencies on the effective Raman detuning, the atom-atom s-wave scattering length, and the intensities of the lasers used for Raman transitions both in GP and MGP approaches. It has been shown that the excitation frequencies depend strongly on these three parameters. Excitation frequencies decrease with the increase in the effective detuning and the s-wave scattering length in general. But the excitation frequencies from the MGP approach differ significantly from the GP results with increase in the s-wave scattering length and show an upward trend for the modes of excitations which depend on the interaction energies for both the traps (axial and spherical). In contrast, the excitation frequencies increase with an increase in the strength of the coupling lasers, manifesting the effect of atom-molecular coupling strength on the excitation frequencies. Since the effective s-wave scattering length increases with laser intensity the effect of higher-order nonlinear interaction becomes prominent with the increase in the laser intensity. It has been shown that the difference between excitation frequencies from GP and MGP approaches increases with the increase in laser intensity. It has been also shown that with the smaller values of detuning and higher values of atom-molecular coupling strength the atom-to-molecule conversion efficiency increases. Consequently, the collective excitation frequencies for hybrid atom-molecule condensates are found to exhibit significant differences from those for the pure atomic BEC results.

ACKNOWLEDGMENTS

We thank D. S. Ray of the Department of Physical Chemistry for useful discussions.

[1] R. Wynar, R. S. Freeland, D. J. Han, C. Ryu, and D. J. Heinzen, Science **287**, 1016 (2000).
[2] K. Winkler, F. Lang, G. Thalhammer, P. v. d. Straten, R. Grimm, and J. H. Denschlag, Phys. Rev. Lett. **98**, 043201 (2007).
[3] J. G. Danzl *et al.*, Science **321**, 1062 (2008).
[4] E. Timmermans, P. Tommasini, R. Cote, M. Hussein, and A. Kerman, Phys. Rev. Lett. **83**, 2691 (1999).
[5] E. Timmermans *et al.*, Phys. Rep. **315**, 199 (1999).
[6] D. J. Heinzen, R. Wynar, P. D. Drummond, and K. V. Kheruntsyan, Phys. Rev. Lett. **84**, 5029 (2000).
[7] F. D. de Oliveira and M. K. Olsen, Opt. Commun. **234**, 235 (2004).
[8] M. Gupta and K. R. Dastidar, Phys. Rev. A **80**, 043618 (2009).
[9] M. Gupta and K. R. Dastidar, Phys. Rev. A **81**, 033610 (2010).
[10] D. S. Jin, J. R. Ensher, M. R. Matthews, C. E. Wieman, and E. A. Cornell, Phys. Rev. Lett. **77**, 420 (1996).

[11] D-M. Stampern-Kurn, H. J. Miesner, S. Inouye, M. R. Andrews, and W. Ketterle, Phys. Rev. Lett. **81**, 500 (1998).
[12] M. O. Mewes, M. R. Andrews, N. J. van Druten, D. M. Kurn, D. S. Durfee, C. G. Townsend, and W. Ketterle, Phys. Rev. Lett. **77**, 988 (1996).
[13] Y. Lu *et al.*, Chin. Phys. Lett. **26**, 076701 (2009).
[14] S. Stringari, Phys. Rev. Lett. **77**, 2360 (1996).
[15] M. Edwards, P. A. Ruprecht, K. Burnett, R. J. Dodd, and C. W. Clark, Phys. Rev. Lett. **77**, 1671 (1996).
[16] V. M. Pérez-García, H. Michinel, J. I. Cirac, M. Lewenstein, and P. Zoller, Phys. Rev. Lett. **77**, 5320 (1996).
[17] F. Dalfovo, S. Giorgini, L. Pitaevskii, and S. Stringari, Rev. Mod. Phys. **71**, 463 (1999), and references in section IV.
[18] A. J. Leggett, Rev. Mod. Phys. **73**, 307 (2001), and references in section IV.
[19] J. O. Andersen, Rev. Mod. Phys. **76**, 599 (2004), and references in section III D.
[20] D. S. Petrov, M. Holzmann, and G. V. Shlyapnikov, Phys. Rev. Lett. **84**, 2551 (2000).
[21] L. Pitaevskii and S. Stringari, Phys. Rev. Lett. **81**, 4541 (1998).
[22] S. Ronen, J. Phys. B: At. Mol. Opt. Phys. **42**, 055301 (2009), and references therein.
[23] A. Banerjee and M. P. Singh, Phys. Rev. A **66**, 043609 (2002).
[24] M. Gupta and K. R. Dastidar, J. Phys. B: At. Mol. Opt. Phys. **41**, 195302 (2008).
[25] M. Gupta and K. R. Dastidar, J. Phys.: Conf. Ser. **80**, 012038 (2007).
[26] C.-Y. Lin, P. Tommasini, E. J. V. de Passos, M. S. Hussein, and A. F. R. de Toledo Piza, Phys. Rev. A **68**, 063615 (2003).
[27] O. Bohigas, A. M. Lane, and J. Martorell, Phys. Rep. **51**, 267 (1971).
[28] E. Lipparini and S. Stringari, Phys. Rep. **175**, 103 (1989).
[29] Y. L. Ma, Eur. Phys. J. D **29**, 415 (2004).
[30] T. Kimura, H. Saito, and M. Ueda, J. Phys. Soc. Jpn. **68**, 1477 (1999).
[31] T. Kimura, Phys. Rev. A **66**, 013608 (2002).
[32] T. Kimura, Physica B **329**, 44 (2003).
[33] N. N. Bogoliubov, J. Phys. (Moscow) **11**, 23 (1947).
[34] T. D. Lee, K. Huang, and C. N. Yang, Phys. Rev. A **106**, 1135 (1957).
[35] M. Theis, G. Thalhammer, K. Winkler, M. Hellwig, G. Ruff, R. Grimm, and J. H. Denschlag, Phys. Rev. Lett. **93**, 123001 (2004).
[36] G. Thalhammer, M. Theis, K. Winkler, R. Grimm, and J. H. Denschlag, Phys. Rev. A **71**, 033403 (2005).